

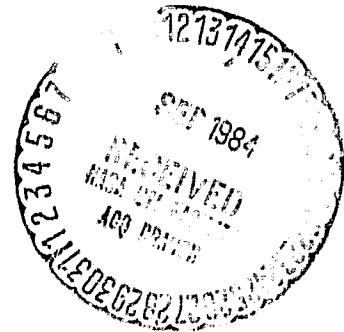
General Disclaimer

One or more of the Following Statements may affect this Document

- This document has been reproduced from the best copy furnished by the organizational source. It is being released in the interest of making available as much information as possible.
- This document may contain data, which exceeds the sheet parameters. It was furnished in this condition by the organizational source and is the best copy available.
- This document may contain tone-on-tone or color graphs, charts and/or pictures, which have been reproduced in black and white.
- This document is paginated as submitted by the original source.
- Portions of this document are not fully legible due to the historical nature of some of the material. However, it is the best reproduction available from the original submission.

RELATIVE RADIOMETRIC CALIBRATION OF LANDSAT
TM REFLECTIVE BANDS
(SUMMARY)

JOHN L. BARKER ✓
NASA/GODDARD SPACE FLIGHT CENTER



INTRODUCTION

The paper summarized herein presents results and recommendations pertaining to characterization of the relative radiometric calibration of the protoflight Thematic Mapper sensor (TM/PF). TM/PF is the primary experiment on the Landsat-4 satellite, launched on July 16, 1982. Some preliminary pre-launch and in-orbit results are also included from the flight model (TM/F) on Landsat-5, which was launched on March 1, 1984. The goals of the paper are:

- Outline a common scientific methodology and terminology for characterizing the radiometry of both TM sensors
- Report on the magnitude of the most significant sources of radiometric variability
- Recommend methods for achieving the exceptional potential inherent in the radiometric precision and accuracy of the TM sensors.

RADIOMETRIC CHARACTERIZATION

The radiometric characteristics of TM digital imagery that are important for scientific interpretation include mean values of absolute and relative calibration constants, and estimates of the uncertainty in the relative and absolute post-calibration radiances. Mean values and uncertainties in the pre-launch absolute radiometric calibration are discussed



elsewhere (Barker, Ball et al., 1984). The subject paper focuses on characterizing variability and uncertainty of TM relative radiometry, including total variability as well as its systematic and random components. Emphasis is placed on identifying the magnitude and types of systematic errors, since these have the potential for being reduced during ground processing. Estimates of innate random variability, such as the standard deviation of a signal or its signal-to-noise ratio, are also important since they place limits on the inferences that can be drawn from single and multiple pixel radiances. However, accurate estimates of random error require the prior removal of all types of systematic variability.

SOURCES OF RADIOMETRIC VARIABILITY

Radiometric variability in the final TM image can be divided into three components, based on origin:

- Scene Variability (the source of potential information)
 - Solar Irradiance
 - Atmospheric Transmission, Absorption and Scattering (Reflection)
 - Transmission, Absorption and Reflection (Scattering) of the Target, including Shadows
- Optical and Electrical Variability of the Sensor
 - Reflected Radiance from the TM Scanning Mirror
 - Radiance from the TM Internal Calibrator (IC)
- Variability Introduced During Processing
 - "Active Scan" Imagery
 - "End-of-Scan" Shutter Calibration Data
 - Housekeeping Telemetry

Once the total variability from all non-information sources is characterized, then an evaluation can be made as to the adequacy of the precision for specific requirements. If the sensor has already been placed in orbit, as with TM/PF and TM/F, then only the systematic errors from the sensor and any possible additional errors introduced by data processing can be reduced.

ORGANIZATION OF PAPER

The table of contents for the paper is given in Table 15 at the end of this summary. Specific objectives of the research effort reported in the paper include:

- Monitoring radiometric performance of TM sensor with time (Sections 2 and 3)
- Characterizing sources of within-scene variability and uncertainty in measuring radiance with the TM sensor (Section 4)
- Outlining possible pre-distribution methodologies for optimizing TM radiometric calibration parameters based on scientific information extraction requirements and on radiometric characteristics of the TM sensor (Section 5)
- Recommending changes in operational or processing procedures and identifying candidates for further calibration, experimentation, and research (Section 6).

APPROACH TO RADIOMETRIC CHARACTERIZATION

The paper concentrates on an analysis of raw TM calibration data from pre-launch tests and from in-orbit acquisitions. A library of approximately one thousand pre-launch test tapes, each of which samples the equivalent of one scene, is currently maintained for characterization. About 25-50% have been examined. Most of the analyses of these tapes, and of data from in-orbit acquisitions, used a software program called TM Radiometric and Algorithmic Performance Program (TRAPP). Required input for TRAPP analyses includes both the raw IC calibration data from the shutter region as well as the raw uncalibrated TM digital imagery. These raw data are not available to the general public. They are used to characterize radiometric characteristics of the sensor rather than performance of the processing system.

The results of the characterization activities reported in the paper (and summarized in the following paragraphs) derive from analyses of raw (IC and image) data only. These results, therefore, pertain to all TM imagery without regard to ground processing system, be it the NASA Scroinge Era (prior to 15 January 1984) system, the TM Image Processing System (TIPS) (effective after 15 January 1984) or other ground processing facilities. Discussion of image processing techniques in response to sensor characteristics will typically reference TIPS but are applicable universally.

CHARACTERIZATION RESULTS

Post Calibration Dynamic Range

Pre-launch absolute radiometric calibrations of the six reflective bands on TM/F were used to identify a pre-calibration range of sensitivity for each of the 96 channels. These results were combined with similar pre-launch calibration ranges of sensitivity for each band in TM/PF to provide a per band post-calibration dynamic range for processing TM imagery on the TIPS. Each post-calibration dynamic range is defined by the minimum spectral radiance, RMIN, and the maximum, RMAX, for the band as given in Table 1. RMIN and RMAX values will be up-dated based on recalibration of the integrating sphere used for pre-launch absolute calibration and on reduction of certain systematic errors in the raw digital data.

Between-Scene Changes in TM/PF Gain

Data on the radiometric stability of the TM/PF with time are recorded for use in future sensor-to-sensor and sensor-to-ground absolute calibration. Figure 1 gives a plot of the band-averaged gain with time for 50 scenes of Band 4. It illustrates the least noisy of the apparent monotonic decreases in IC-determined gain for the four bands on the Primary Focal Plane (PFP). One hypothesis is that this asymptotic drop of 3 to 6% during 300 days in orbit is a long-term "vacuum shift" curve. Vacuum shift has traditionally referred to the difference between IC pulses measured during pre-launch absolute calibration under ambient atmospheric conditions and the IC pulse values observed during pre-launch thermal vacuum testing. This justifies the use of

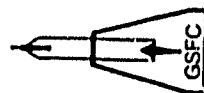
TABLE 1.

**TM POST-CALIBRATION DYNAMIC RANGE IN
SPECTRAL RADIANCE
(mW cm⁻² ster⁻¹ μm⁻¹)
(FOR TM DIGITAL IMAGERY PROCESSED ON TIPS
AFTER 15 JAN 84)**

	BAND 1 BAND 2 BAND 3 BAND 4 BAND 5 BAND 7						
RMIN ^a AT L _{cal} =0 DN	-0.15	-0.28	-0.12	-0.15	-0.037	-0.015	
RMAX ^b AT L _{cal} =255 DN	15.21	29.68	20.43	20.62	2.719	1.438	

$${}^a\text{RMIN} = \frac{-0^\circ \text{ (B)}}{G^\circ \text{ (B)}} \qquad {}^b\text{RMAX} = \frac{\text{RANGE} - 0^\circ \text{ (B)}}{G^\circ \text{ (B)}}$$

$$L_\lambda = \frac{L_{\text{cal}} - 0^\circ \text{ (B)}}{G^\circ \text{ (B)}} = \text{RMIN} + \left[\frac{\text{RMAX} - \text{RMIN}}{\text{RANGE}} \right] L_{\text{cal}}$$

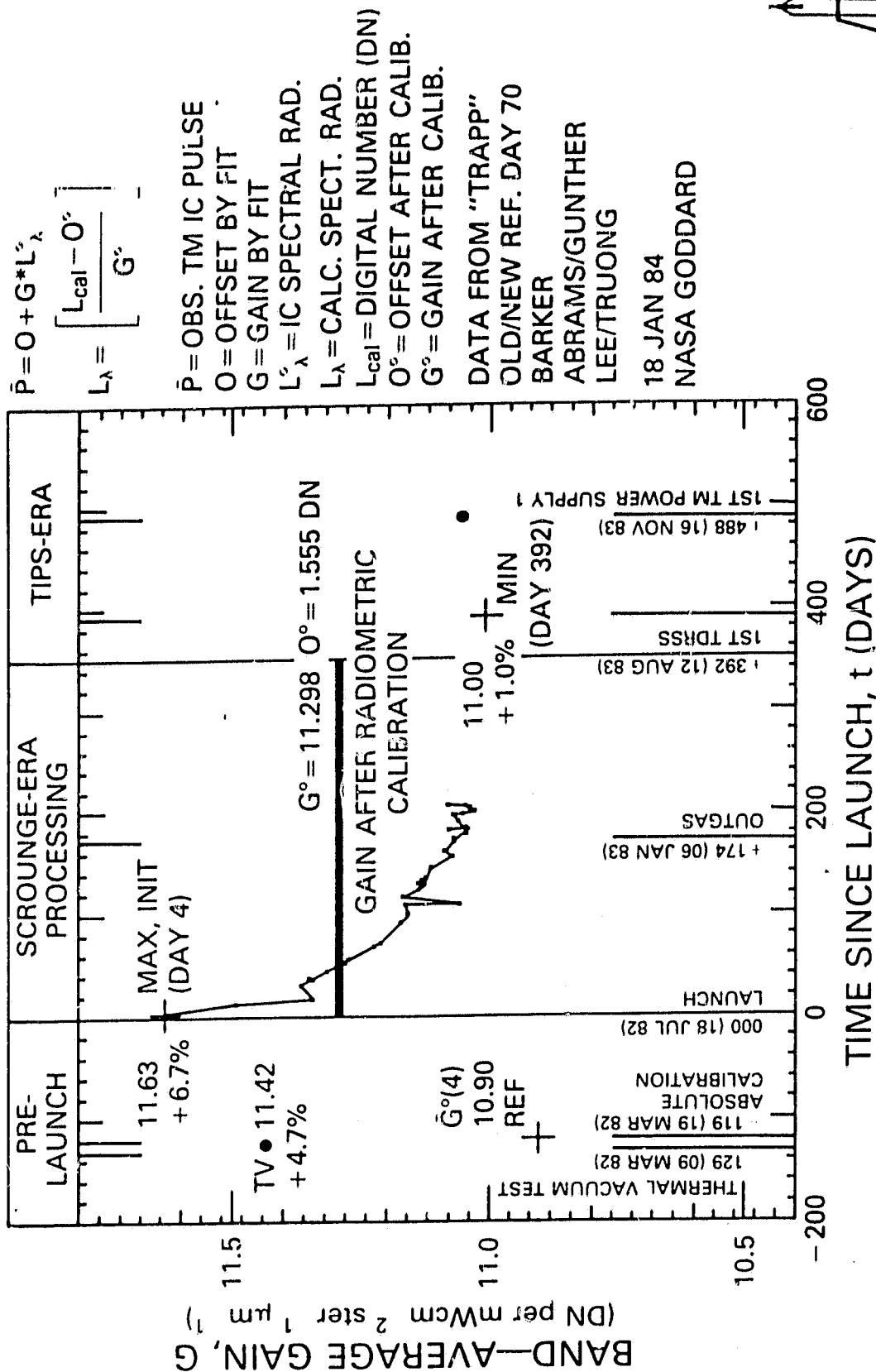


BARKER APR 84

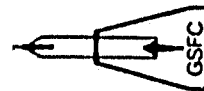
FIGURE 1.

LANDSAT-4 TM RADIOMETRY, BAND 4

APPARENT GAIN CHANGES FROM INTERNAL CALIBRATOR (IC) PULSES



ORIGINAL PAGE IS
OF POOR QUALITY



BARKER APR 84 GSFC

IC pulses for radiometric calibration of the PFP under the assumption that the "vacuum shift" is due to an optical, physical, or electrical property of the detector and channel itself, rather than to some characteristic of the IC system.

Figure 2 is a plot of the band-averaged gain for Band 5 with time. The cyclic pattern has a period of 54 days, with an rms uncertainty of about 2 days. A similar, although less well defined cyclic pattern is observed in the other shortwave infrared (SWIR) band, i.e., Band 7 has a period of 75 days with a rms error of about 6 days. Differences between peaks and valleys is always less than 9% for both SWIR bands.

The origin of these cyclic patterns on the Cold Focal Plane (CFP) is not known. One hypothesis, based on the apparent direct relationship of the periods and the wavelengths of the SWIR bands, is that the CFP and its optics are moving at a fixed rate of 11 nm/yr relative to the lens on the shutter and the PFP. This hypothesis is possible since the relay optics containing the CFP were designed to be moved in order to bring it into focus with the PFP. Since the velocity of a wave is equal to its wavelength divided by its period, the observed periods for Bands 5 and 7 both imply a velocity of 11 nm/yr. An additional hypothesis is required to explain the amplitude of the cyclic patterns. One such hypothesis is that the amplitude is a function of how close the optics are to the diffraction limit, where it will vary with phase. One test of these hypotheses would be to look for a cyclic pattern in the third band on the CFP, namely the thermal band, and relate its period to its wavelength. Similarly the hypothesized cyclic Band 6 variation in amplitude should depend on the relative sizes and areas of the detectors on the CFP as well as their wavelengths. Proof of this model for the cyclic pattern of the SWIR bands will call for the continued use of the IC to calibrate these bands.

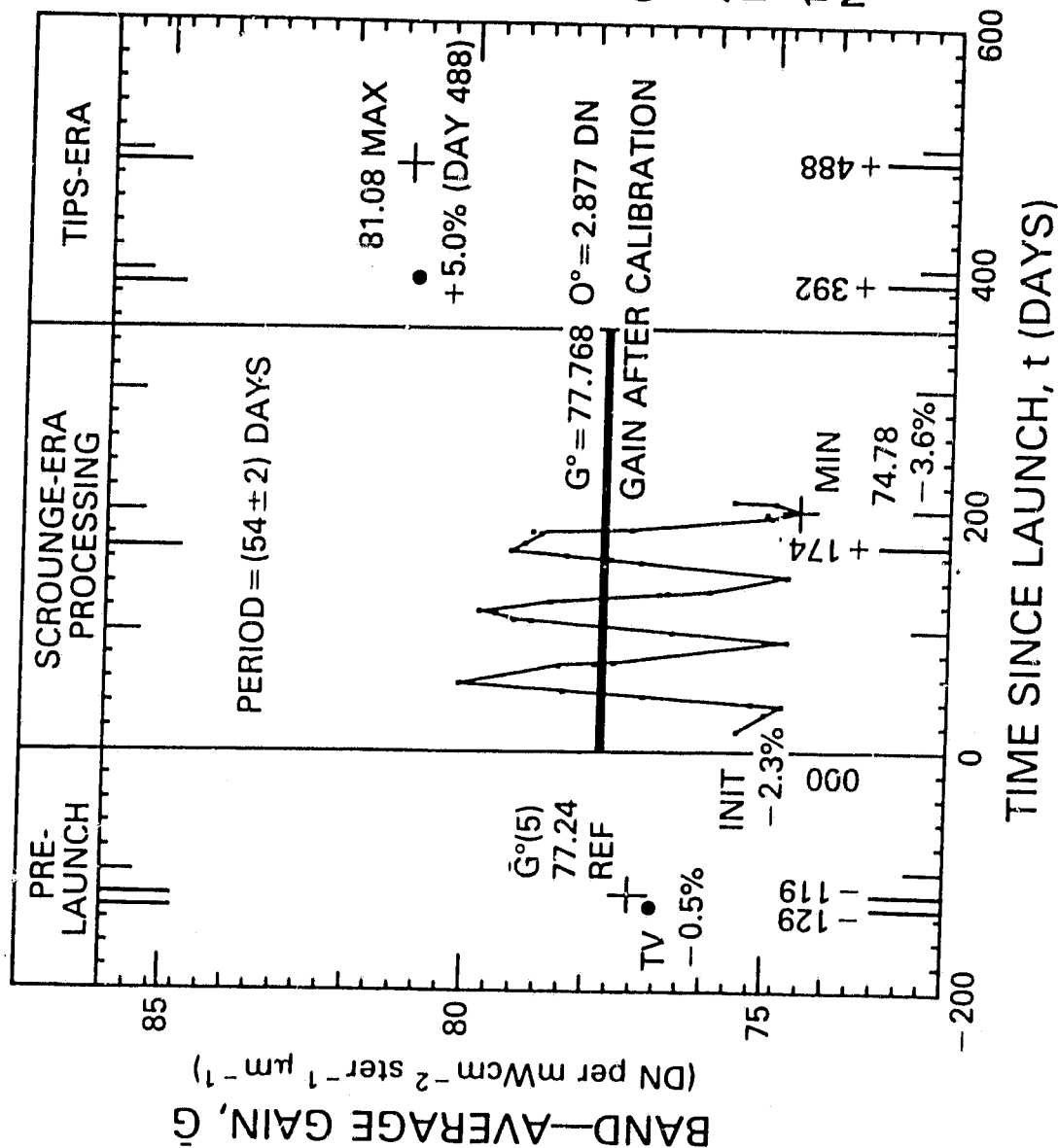
Assuming perfect operation of the IC, all of these slowly varying trends in gain have been corrected out during the calibration of the TM imagery.

FIGURE 2.

$$\begin{aligned} \bar{P} &= O + G * L_{\lambda} \\ L_{\lambda} &= \left[\frac{L_{cal} - O^{\circ}}{G^{\circ}} \right] \\ \bar{P} &= \text{OBS. TM IC PULSE} \\ O &= \text{OFFSET BY FIT} \\ G &= \text{GAIN BY FIT} \\ L_{\lambda}^{\circ} &= \text{IC SPECTRAL RAD.} \\ L_{\lambda} &= \text{CALC. SPECT. RAD.} \\ L_{cal} &= \text{DIGITAL NUMBER (DN)} \\ O^{\circ} &= \text{OFFSET AFTER CALIB.} \\ G^{\circ} &= \text{GAIN AFTER CALIB.} \end{aligned}$$

DATA FROM "TRAPP"
OLD/NEW REF. DAY 70
BARKER
ABRAMS/GUNTHER
LEE/TRUONG

18 JAN 84
NASA GODDARD



There is an approximately 0.5% rms range of variability around these smoothly varying curves of band-averaged gain versus time for bands 4 and 5. While the individual curves of IC-determined gain versus time for each individual channel appear to be even more well defined, the statistical square root of 16 channels indicates that the radiometric predictability of individual channels is at least better than rms error of 0.2%. This radiometric reproducibility of the TM sensor in space suggests that systematic corrections during the ground processing of TM imagery will significantly improve radiometry.

Between-Band Changes in TM/PF Gain

In addition to maintaining scene-to-scene calibration of each band, it is also necessary to maintain band-to-band calibration. Current TIPS procedures do not provide for any within-band or between-band correlation of channels. One limit on the possible between-band variability is change in absolute gain on each of the individual bands. Apparent change in TM/PF gain, relative to the gain determined during pre-launch absolute calibration, are summarized for four specific times in Table 2. The first time was a pre-launch Thermal Vacuum (TV) test, which was designed to duplicate conditions expected in space. The second time was the actual initial (INIT) in-orbit measurement on that band. The difference between these two changes in gain (INIT-TV) was equal to or less than 2% and is a measure of how well the pre-launch TV tests agreed with the first measurements in space. The third and fourth times were upon occurrence of the maximum and minimum values of the IC-determined gain observed over the first year that Landsat-4 was in space. The range of change (MAX-MIN) is an indication of a possible uncertainty of 3 to 9% in the absolute radiometric calibration of the TM/PF reflective bands. The differences between MAX-MIN values for the bands in Table 1 are measures of the limits on possible differences in band-to-band calibrations with time. If the IC system has been working as designed then the radiometric calibration of TM imagery with the IC data will maintain the absolute calibration of the bands, and therefor will also maintain the band-to-band calibration.

TABLE 2.

APPARENT CHANGES IN TM/PF GAIN.

BAND REF, \bar{G}°	RELATIVE CHANGE IN %, 100 $\left[\frac{\bar{G} - \bar{G}^\circ}{\bar{G}^\circ} \right]^*$						
	1	2	3	4	5	7	
TV (PRE-LAUNCH)	15.78	8.10	10.62	10.90	77.24	147.12	
INIT (IN-ORBIT)	-1.2	-1.0	3.2	4.7	-0.5	-0.5	
(INIT-TV)	-1.1	-1.0	3.6	6.7	-2.3	-0.8	
	0.1	0.0	0.5	2.0	-1.8	-0.3	
MAX (IN-ORBIT)	-1.1	-1.0	3.6	6.7	5.0	3.3'	
MIN (IN-ORBIT)	-8.2	-4.5	-2.8	1.0	-3.6	-2.5	
MAX-MIN	7.1	3.4	6.5	5.7	8.5	5.8	

*GAINS CALCULATED FROM LANDSAT-4 TM/PF INTERNAL CALIBRATION (IC) PULSES, \bar{P} , REGRESSED AGAINST IC EFFECTIVE SPECTRAL RADIANCE, L_λ° :

$$\bar{P} = 0 + G \cdot L_\lambda^\circ$$

WHERE 0 IS FITTED OFFSET AND G IS FITTED GAIN FOR A CHANNEL.

BAND-AVERAGE GAINS, \bar{G} , ARE COMPARED TO AN AMBIENT ABSOLUTE CALIBRATION REFERENCE G° OF 19 MARCH 1982, WHERE GAINS ARE IN DN per mWcm^{-2} ster $^{-1}\mu\text{m}^{-1}$.



BARKER
FEB 84

Within-Scene Variability in TM Radiometry

If radiometric calibration is done on one scene at a time, as is the case with Scrounge era and TIPS processing, then any sources of systematic variation which occur during the 23 seconds it takes to acquire a scene will remain uncorrected. During initial studies of TM imagery, the following types of within-scene variability have been identified:

- **Bin-Radiance Dependence.** The mean value of any specific digital number (DN) can be mislocated by up to two levels. Additionally, bin widths vary from nearly zero to 2 DN values. Both effects are due to errors in the analog-to-digital (A/D) converter's bin sizing and location (threshold voltages). Therefore, a calibration which uses more than the 8 bits of the original data can be used to more accurately estimate the mean value of the observed radiance, especially during the calibration, prior to preparing an 8-bit product tape.
- **Scan-Correlated Shifts** (discussed below).
- **Coherent Noise** (discussed below).
- **Within-Line Droop.** "Droop" is one of 3 types of "within-line, sample-location dependent noise." By comparing forward west-to-east scans to reverse east-to-west scans, a systematic droop of up to 1 DN was seen in Band 1 of TM/PF. There is a possibility that droop is actually the same as one of the other types of within-line systematic variation, namely Bright-Target Saturation.
- **Bright-Target Saturation** (discussed below).
- **Forward/Reverse-Scan Difference.** Apparent differences between forward and reverse scans may actually be related to the last exposure to a bright target. If an image contains bright objects, which are not symmetric on a scan-by-scan basis

relative to beginning and end of obscuration of the optical axis by the calibration shutter, then bright-target saturation effects will cause an apparent difference in the average values for the forward and reverse scans for the whole scene.

Reference Channels for the TM Sensors

Different channels within a band show different magnitudes for the various sources of within-scene variability. Furthermore, the random noise in the noisiest channel can be as much as a factor of two higher than in the quietest channel. Those channels with the lowest apparent rms noise on the shutter are given in Table 3. Channels with the highest rms noise, highest value for scan-correlated shift, and highest value for coherent noise are also listed. Bright-target saturation appears to have approximately the same effect on all channels in a band, probably because it is a characteristic of the design of the electronics. The high-noise reference channels may be useful for serial stripping of various types of within-scene noise. Magnitudes for these sources of TM radiometric variability are given in Table 4 for each of the reference channels currently identified on Landsat-4 TM/PF and Landsat-5 TM/F.

Scan-Correlated Shifts

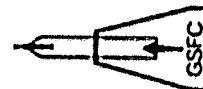
Scan-correlated shifts are one of two types of "between-scan line-independent noise"; the other type being differences between forward and reverse scans. These shifts are defined by the observed discontinuity in background level. Three most significant examples are discussed as types 4-1, 4-7 and 5-3 to indicate the satellite and band in which they occur. A procedure for correcting for scan-correlated shifts has been developed and tested as part of this study. Assumptions made include:

- Shifts are constant within a line
- Signed magnitude is consistent within a scene
- Signed magnitude is channel specific

TABLE 3.

TM RADIOMETRIC REFERENCE CHANNELS

	BAND BAND BAND BAND BAND BAND					
	1	2	3	4	5	6
LANDSAT-4 TM/PF						
LOWEST NOISE						
SHUTTER rms	9	14	12	7	2	15 4F
HIGHEST NOISE						
SHUTTER rms	16	2	1	8	7	1
SHIFT TYPE 4-1	4	—	1	16	15	—
SHIFT TYPE 4-7	—	1	16	—	10	7
32 KHz (3.2 mf)	16	6	8	8	[8]	[10]
6 KHz (18 mf)	4	1	1	16	[7]	[7]
LANDSAT-5 TM/F						
LOWEST NOISE						
SHUTTER rms	15	10	2	1	2	15 4
HIGHEST NOISE						
SHUTTER rms	4	1	12	3	10	9 1
SHIFT TYPE 5-3	10	1	1	1	3	—

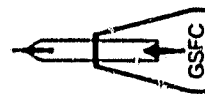


BARKER APR 84

TABLE 4.

TM RADIOMETRIC VARIABILITY (IN DN)

BAND 1 BAND 2 BAND 3 BAND 4 BAND 5 BAND 7						
LANDSAT-4 TM/PF LOWEST NOISE SHUTTER rms	±1.1	±0.4	±0.4	±0.3	±0.8	±0.8
	±1.5	±1.0	±1.3	±0.6	±1.1	±2.0
	2.0	—	0.3	0.2	-0.1	—
	—	-0.2	0.6	—	0.6	0.9
	2.6	0.3	1.6	0.8	[0.2] [0.3]	[0.3]
HIGHEST NOISE SHUTTER rms SHIFT TYPE 4-1 SHIFT TYPE 4-7 32 KHz (3.2 mf) 6 KHz (18 mf)	0.4	0.2	0.5	0.3	[0.2] [0.2]	[0.2]
LANDSAT-5 TM/F LOWEST NOISE SHUTTER rms	±0.8	±0.2	±0.5	±0.2	±0.8	±0.8
	±1.0	±0.5	±0.7	±0.5	±1.3	±1.3
	-0.3	0.7	0.5	0.4	—	—



- All channels shift together within a scan
- Different shift types can occur in each band
- Backgrounds are not constant within a line or between lines because of effects such as bright-target saturation. In this study, two regions were used on the shutter to monitor background; "shutter background 1" was an average of 24 or 28 pixels before dark current (DC) restoration, and "shutter background 2" was an average of 24 or 28 pixels after DC restore. Forward and reverse scans were separated, giving four sets of backgrounds:

BF-BDC = Background Forward Before DC

BF-ADC = Background Forward After DC

BR-BDC = Background Reverse Before DC

BR-ADC = Background Reverse After DC.

Steps in the procedure for scan-correlated shift correction include:

- Separately process forward and reverse scans
- Use a reference channel for each type of shift:
 - Type 4-1 = Landsat-4, Band 1, Channel 4
 - Type 4-7 = Landsat-4, Band 7, Channel 7
 - Type 5-3 = Landsat-5, Band 3, Channel 1
- Use shutter background to monitor shifts
- Create a binary mask indicating the presence or absence of each type of shift in each scan
- Calculate the averaged signed magnitude of shift in each channel for each type of shift by averaging the differences between backgrounds at each binary transaction
- Apply corrections on a line-by-line basis.

For Landsat-4 TM/PF, the 12 August 1983 scene of San Francisco, CA (40392-18152) was used to illustrate the two most significant types of corrections for scan-correlated shifts. Plots were made of line-averaged background before DC restore, BR-BDC, versus scan number for reverse scans. Plots were made before and after correction for all channels in Band 1 (Figure 3), and for all channels in Band 7 (Figure 4). Signed magnitudes of Type 4-1 shifts, also called "shift 1" or "form 1" shifts, are given in DN units next to the corrected background plots of Band 1 in Figure 3. There were approximately 70 transitions of Type 4-1 in the 380 scans. Type 4-1 shifts are not present in all scenes. Signed magnitudes for Type 4-7 shifts, also called "shift 2" or "form 2" shifts, are given next to the corrected plots of Band 7 in Figure 4. Type 4-1 shifts are as large as 2 DN.

For Landsat-5 TM/F, a 5 March 1984 in-orbit scene of clouds over the Atlantic Ocean (50005-16227) is used to illustrate the single most significant Type 5-3 shift. Plots were made of shutter background BF-BDC, versus scan number before and after correcting all channels in Band 3 (Figure 5). While the magnitude of the largest shifts is lower on TM/F than on TM/PF, shifts are more uniformly present on Landsat-5 TM/F, especially in Bands 2 and 3.

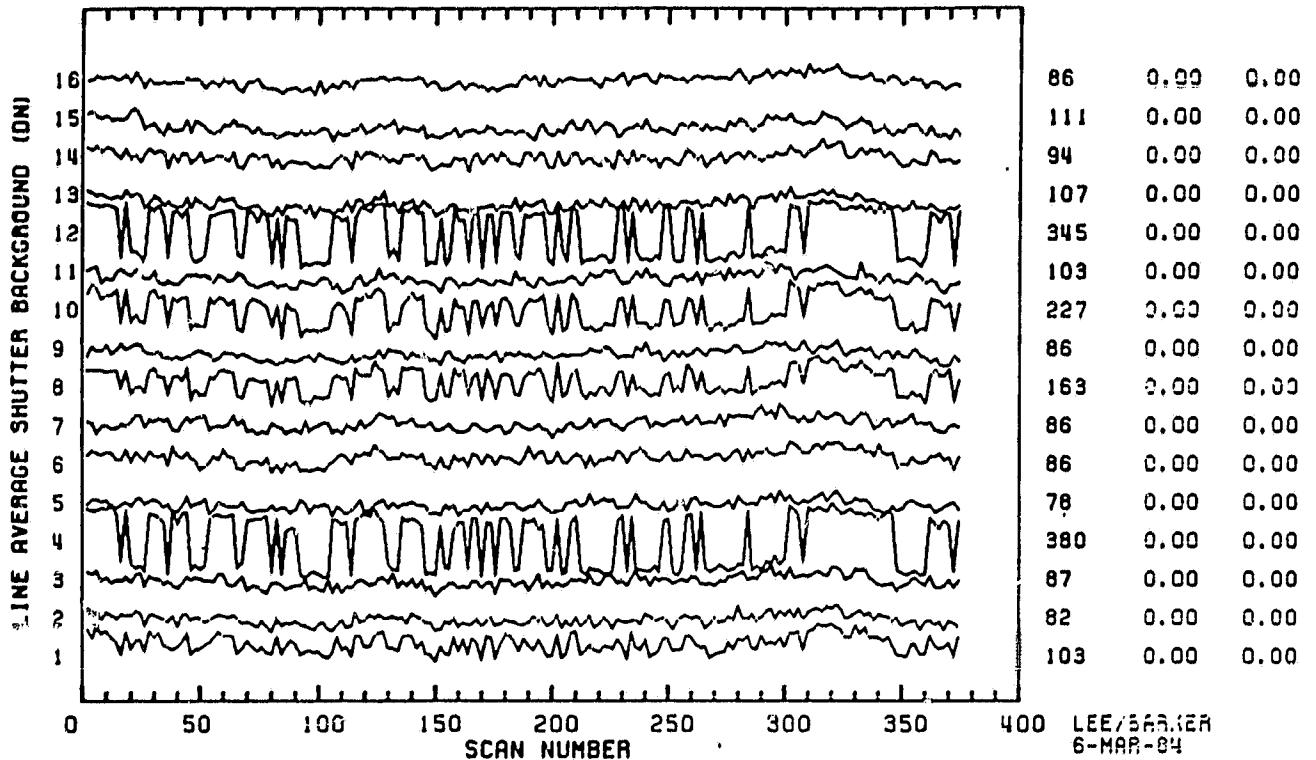
Coherent Noise

Coherent Noise is a "within-scan, sample-location dependent noise", which was made more easily quantifiable in this study by performing a Fast Fourier Transform (FFT) on 512 minor frames (mf) of shutter data from the 3 January 1983 scene of White Sands, NM (approximate ID = 40171-17080; there is no payload correction for this scene so scene ID calculation is approximate). TM/PF exhibits coherent noise in the PFP bands at two frequencies, 32.8 KHz with a period of every 3.2 pixels, and 5.9 KHz with a period of 17.6 pixels. Amounts of coherent noise vary depending on the channel, with the largest integrated area under the 32 KHz peak being about 2.6 DN for Channel 16 of Band 1. Both types of coherent noise in Landsat-4 TM/PF form sharp peaks for PFP bands.

FIGURE 3.

SCENE ID=40392-18152, BAND 1 (REVERSE)
SHUTTER BACKGROUND 1 SPECTRA BEFORE CORRECTION

1000*CV SHIFT1 SHIFT2



SCENE ID=40392-18152, BAND 1 (REVERSE)
SHUTTER BACKGROUND 1 SPECTRA AFTER CORRECTION

1000*CV SHIFT1 SHIFT2

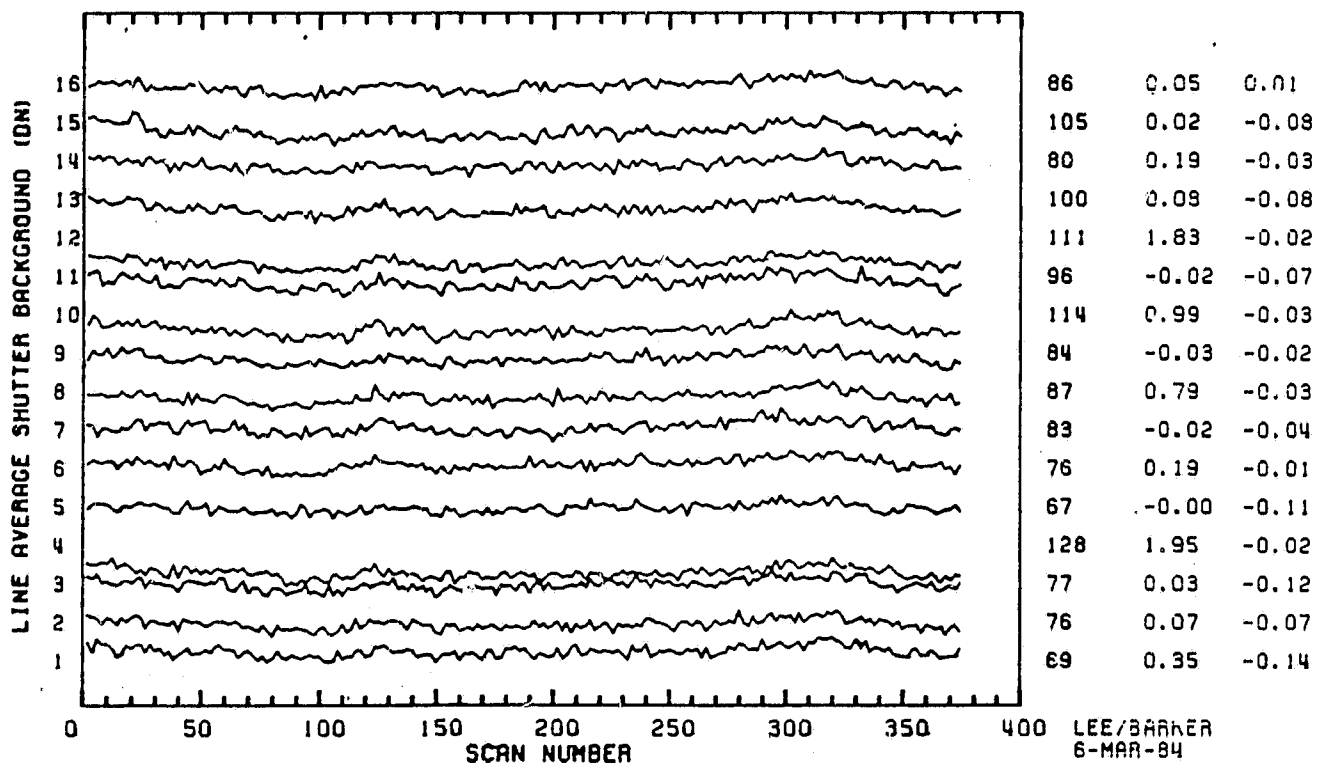
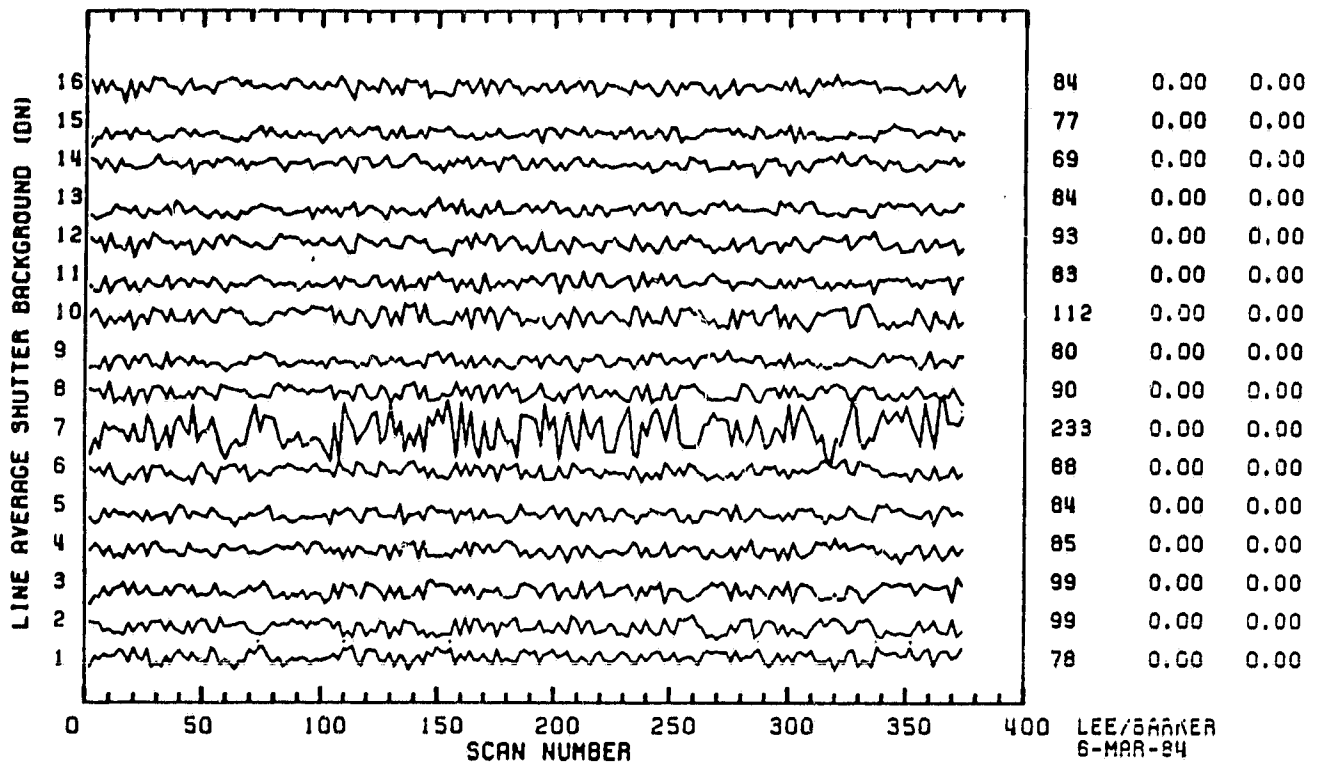


FIGURE 4.

ORIGINAL PAGE NO
OF POOR QUALITY

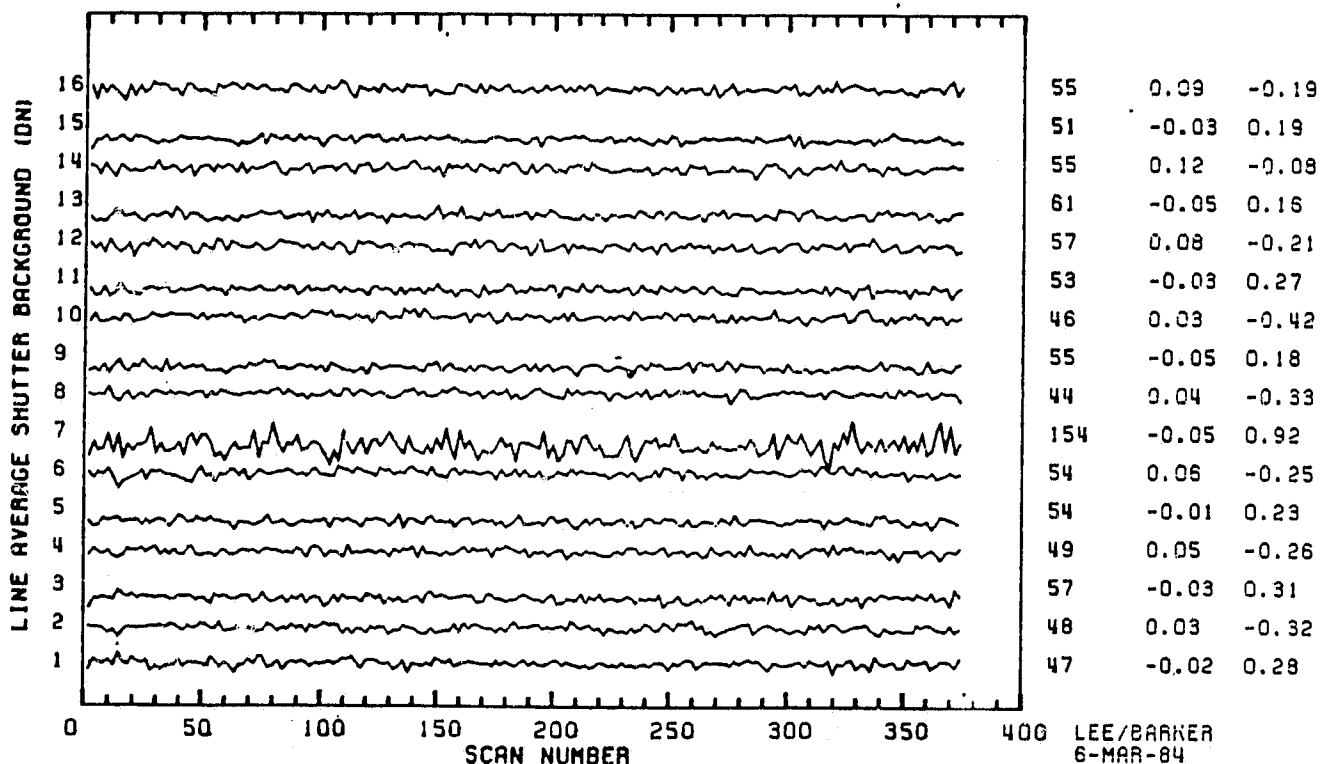
SCENE ID=40392-18152, BAND 7 (REVERSE)
SHUTTER BACKGROUND 1 SPECTRA BEFORE CORRECTION

1000*CV SHIFT1 SHIFT2



SCENE ID=40392-18152, BAND 7 (REVERSE)
SHUTTER BACKGROUND 1 SPECTRA AFTER CORRECTION

1000*CV SHIFT1 SHIFT2

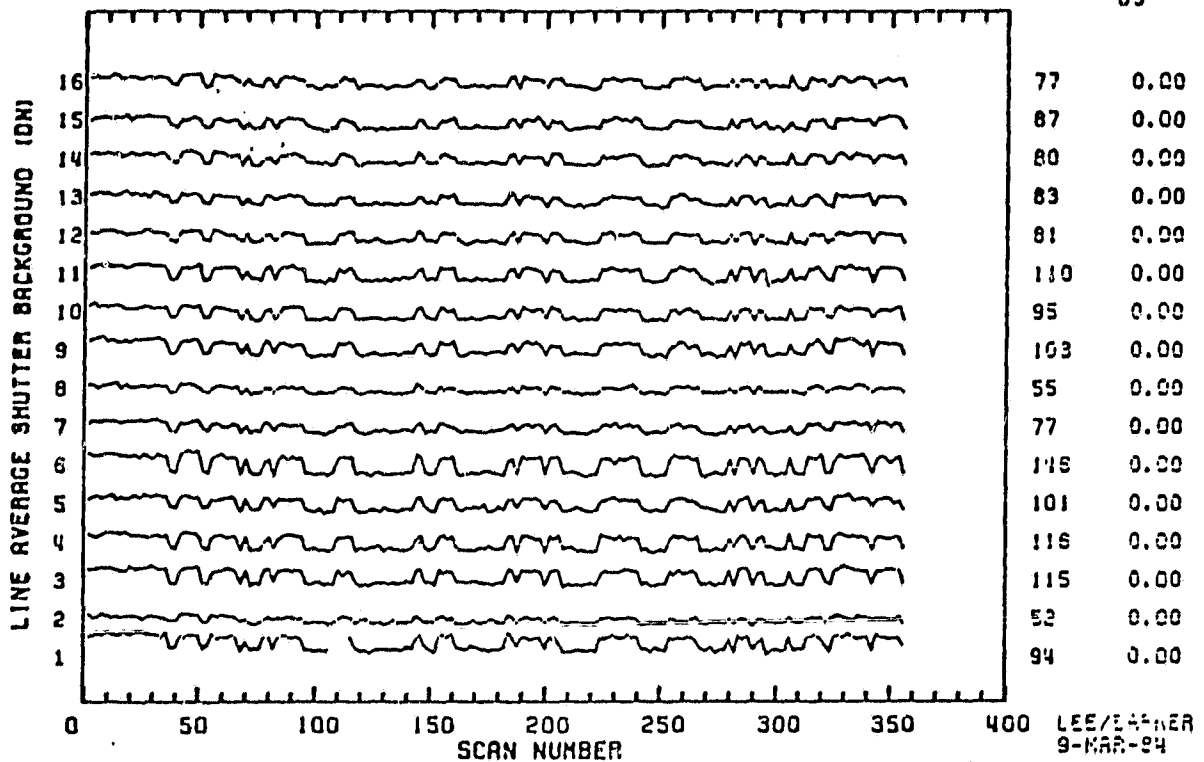


ORIGINAL QUALITY
OF POOR QUALITY

FIGURE 5.

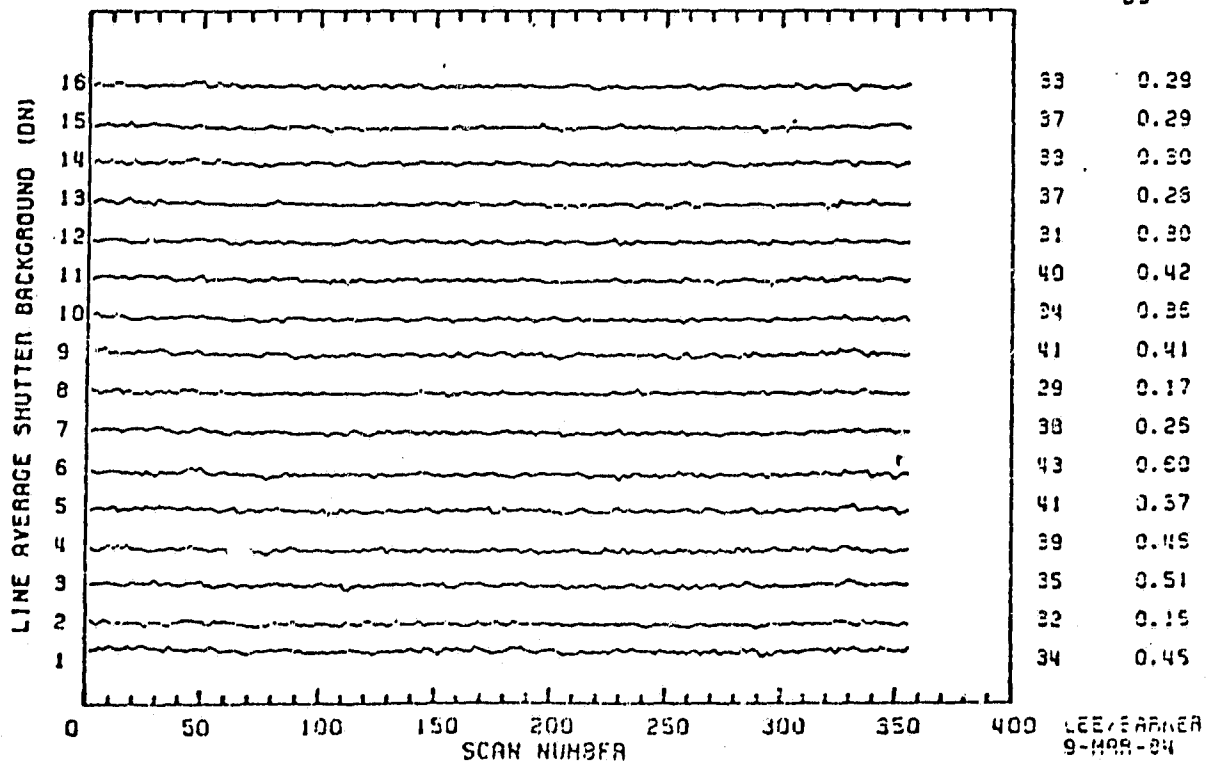
SCENE ID=50005-16221, BAND 3 (FORWARD)
SHUTTER BACKGROUND 1 SPECTRA BEFORE CORRECTION

1000-CV SHIFT
B3



SCENE ID=50005-16221, BAND 3 (FORWARD)
SHUTTER BACKGROUND 1 SPECTRA AFTER CORRECTION

1000-CV SHIFT
B3



Landsat-5 TM/F has a different coherent noise pattern. It does not have a significant peak at 32 KHz. Most channels on the primary focal plane have only one peak, or multiples of it, near 8.5 KHz. This gives spatial periods of every 12.5 pixels, or integer fractions of 12.5 pixels.

Total Within-Scene Variability

An average of the standard deviation of background on the shutter in "quiet scenes" for all channels in a band is given in Table 5 for both TM/PF and TM/F, in units of rms DN. An approximate estimate of the total range of uncertainty for raw radiance values near background can be made by multiplying the total rms noise by six, i.e., ± 3 standard deviations. The uncertainty will be greater at the upper end of the dynamic range. The range of uncertainty is at a low of about 3 DN in Band 4 for both sensors, and at a high of about 7 DN in Band 1 of TM/PF, for these two "quiet" scenes.

The average difference between background in forward and reverse scans in these quiet scenes is less than about 0.2 DN for both sensors. This is part of the justification for suggesting that apparent forward-reverse differences may be related to effects such as bright-target saturation rather than to the direction of scan.

Bright-Target Saturation

Bright-target saturation is like coherent noise and droop in being a "within-line sample-location dependent noise." It is characterized by a memory effect after exposure to a bright target, such as a cloud. The time constant of the hysteresis is such that the effect may last for thousands of samples. There may be two separate physical effects on the detectors, one which has a shorter time constant and decreases the detector sensitivity, and the other which has a longer time constant and increases the sensitivity.

In order to facilitate the interpretation of data in terms of bright-target saturation, a TM scene was chosen which had one "solid" formation of clouds, namely the 12 August 1983 scene of San Francisco, CA (40392-18152). A solid formation of clouds along the coast of the Pacific

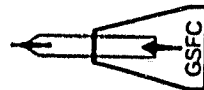
TABLE 5.

WITHIN-SCENE VARIABILITY
TM SHUTTER BACKGROUND IN "QUIET" SCENES
TM/PF ON LANDSAT-4 AND TM/F ON LANDSAT-5
(AVERAGE OF ALL CHANNELS IN A BAND)

BAND	TOTAL VARIABILITY (SD) (FWD-REV) DIFFERENCE		
	TM/PF ^a (DN)	TM/F ^b (DN)	TM/F ^b (DN)
1	±1.24	±0.89	0.04
2	±0.56	±0.29	0.06
3	±0.73	±0.51	0.03
4	±0.41	±0.37	0.01
5	±0.89	±0.93	0.08
7	±1.03	±0.93	0.10

^aLANDSAT-4 IN-ORBIT NIGHT SCENE OF BUFFALO, NY (40037-02243, 22 AUG 82)

^bLANDSAT-5 PRE-LAUNCH AMBIENT INTEGRATING SPHERE (5-198-10563, 30 AUG 83)



BARKER APR 84

Ocean is present on the western side of this scene. It starts about scan 80 and then reaches eastward until there is nearly 75% cloud-cover in the lower quarter of the scene. If there were no bright-target saturation effects, then the background in the shutter region may have the same total rms variability as seen in the quiet scene (Table 5), the same near zero values for the difference between forward and reverse scans, and an independence from scan number after correction for scan-correlated shifts. This may in fact be the case for the SWIR bands, however PFP bands show an increase of about 0.5 DN in rms variability on the shutter, and up to a 2.5 DN difference for forward minus reverse background after DC restore in Band 2 (Table 6). This increases the uncertainty in the calibration of the raw radiance to a range of from 6 to 9 DN, and introduces a scene-dependence on this uncertainty. In addition, the four background plots of shutter background versus scan number in Figures 6 and 7 show a direct relationship with the distribution of the clouds.

One model for bright-target saturation effects relates them to the distance from the end of bright target, or cloud. This hypothesis was tested in this study and the results are shown in Figure 8, where the backgrounds from all four regions on the shutter are plotted against the distances from the cloud edge. The initial 1000 mf undershoot and a 6000 mf overshoot suggests that all of this background data can be fit on a single slowly varying curve, thereby justifying the two component model mentioned above.

Within-Scene Variability by Channel

Examples of the magnitudes of the various types of noise in the TM sensors are summarized by channel in Tables 7 through 13.

RECOMMENDATIONS

While the recommendations listed in summary form in Table 14 contain ideas from many people, including scientific investigators on NASA's team for characterizing the quality of the imagery from the sensors on Landsat-4 and Landsat-5, they are the creation and sole responsibility of the author. These recommendations have not been approved by either the Landsat Science Office or

TABLE 6.

WITHIN-SCENE VARIABILITY
TM SHUTTER BACKGROUND IN CLOUDY SCENE
CLOUDS ON WESTERN EDGE OF SCENE
SAN FRANCISCO, CA (40392-18152, 12 AUG 83)
(AVERAGE OF ALL CHANNELS IN A BAND)

BAND	TOTAL VARIABILITY (SD) (FWD-REV) DIFFERENCE BEFORE AND AFTER DC RESTORE BEFORE AND AFTER DC RESTORE		
	B-BDC (DN)	B-ADC (DN)	B-BDC (DN)
1	± 1.45	± 1.42	1.53
2	± 1.11	± 1.51	2.56
3	± 1.24	± 1.46	2.44
4	± 0.71	± 1.02	1.62
5	± 0.93	± 0.89	0.02
7	± 1.05	± 1.01	0.05



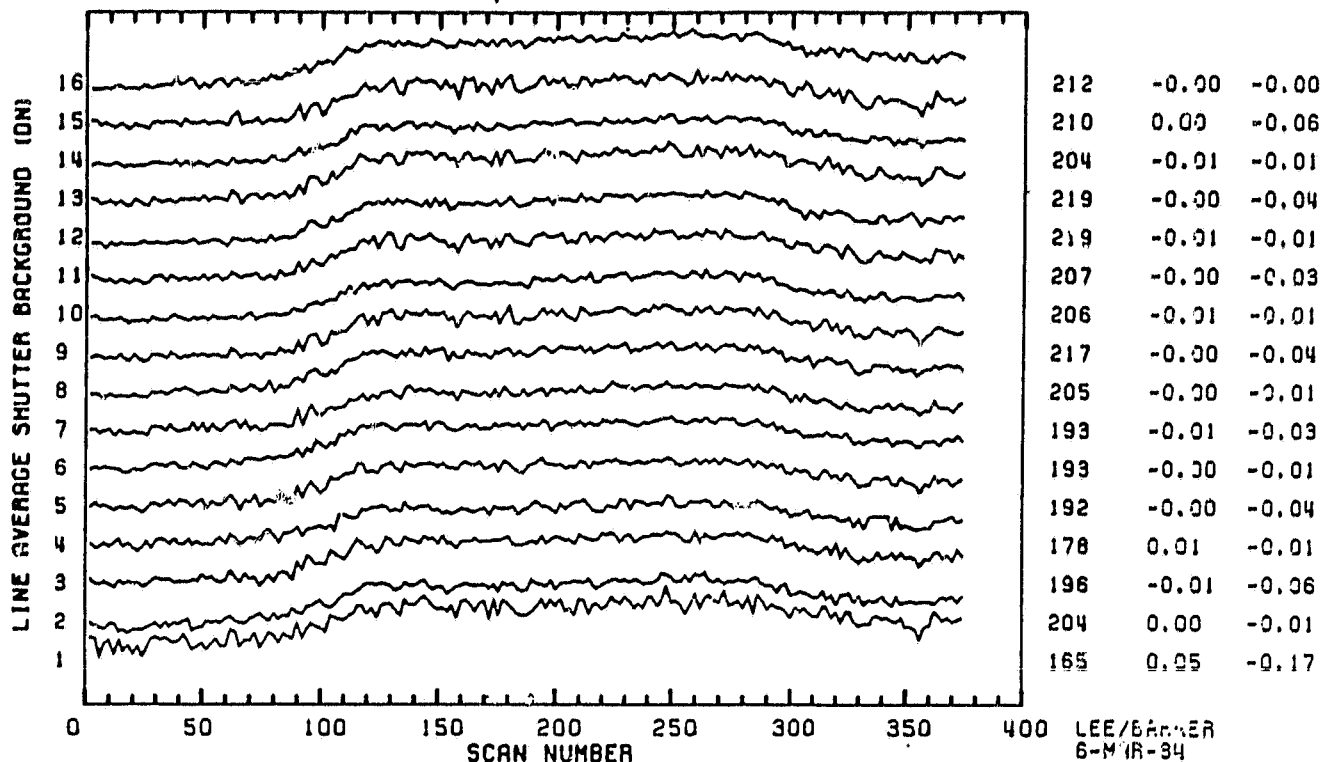
BARKER APR 84 GSFC

FIGURE 6.

ORIGINAL PAGE IS
OF POOR QUALITY

SCENE 10-40392-18152, BAND 2 (FORWARD)
SHUTTER BACKGROUND 1 SPECTRA AFTER CORRECTION

1000*CV SHIFT1 SHIFT2



SCENE 10-40392-18152, BAND 2 (REVERSE)
SHUTTER BACKGROUND 1 SPECTRA AFTER CORRECTION

1000*CV SHIFT1 SHIFT2

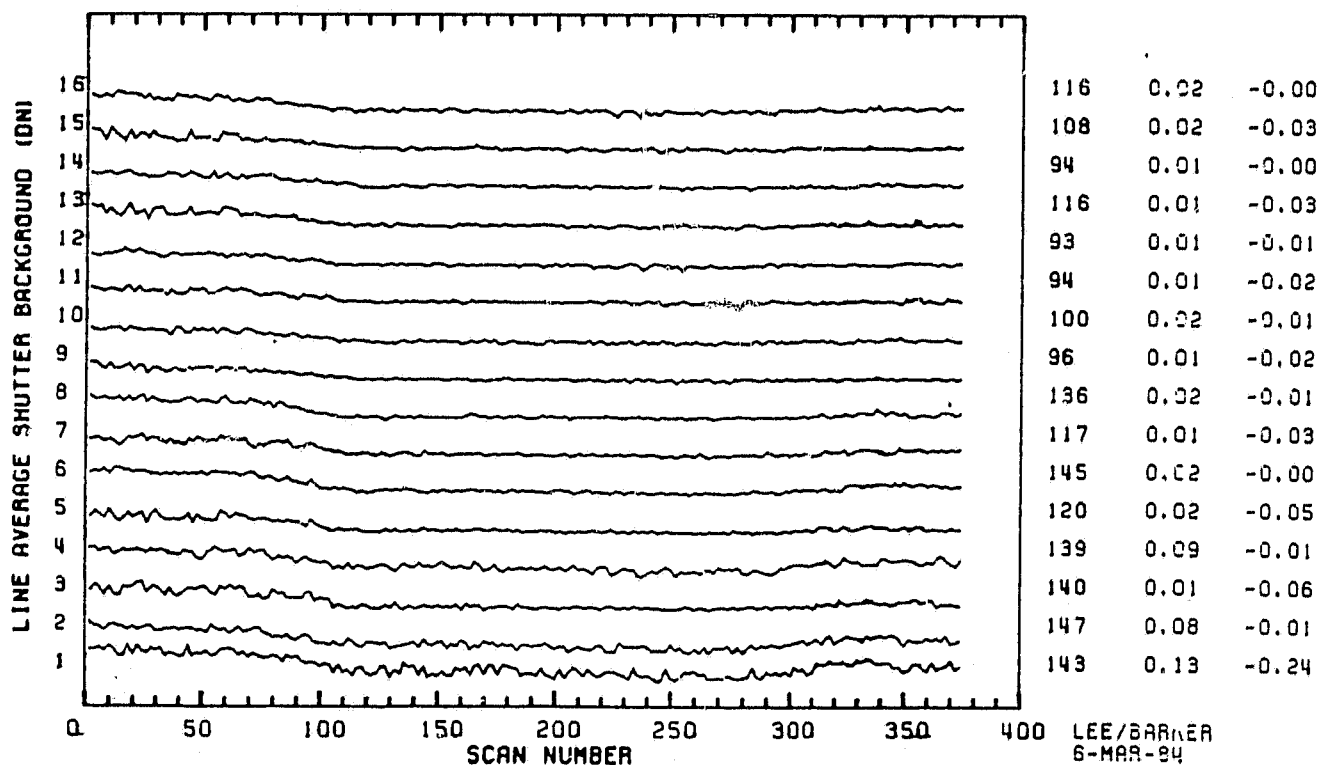
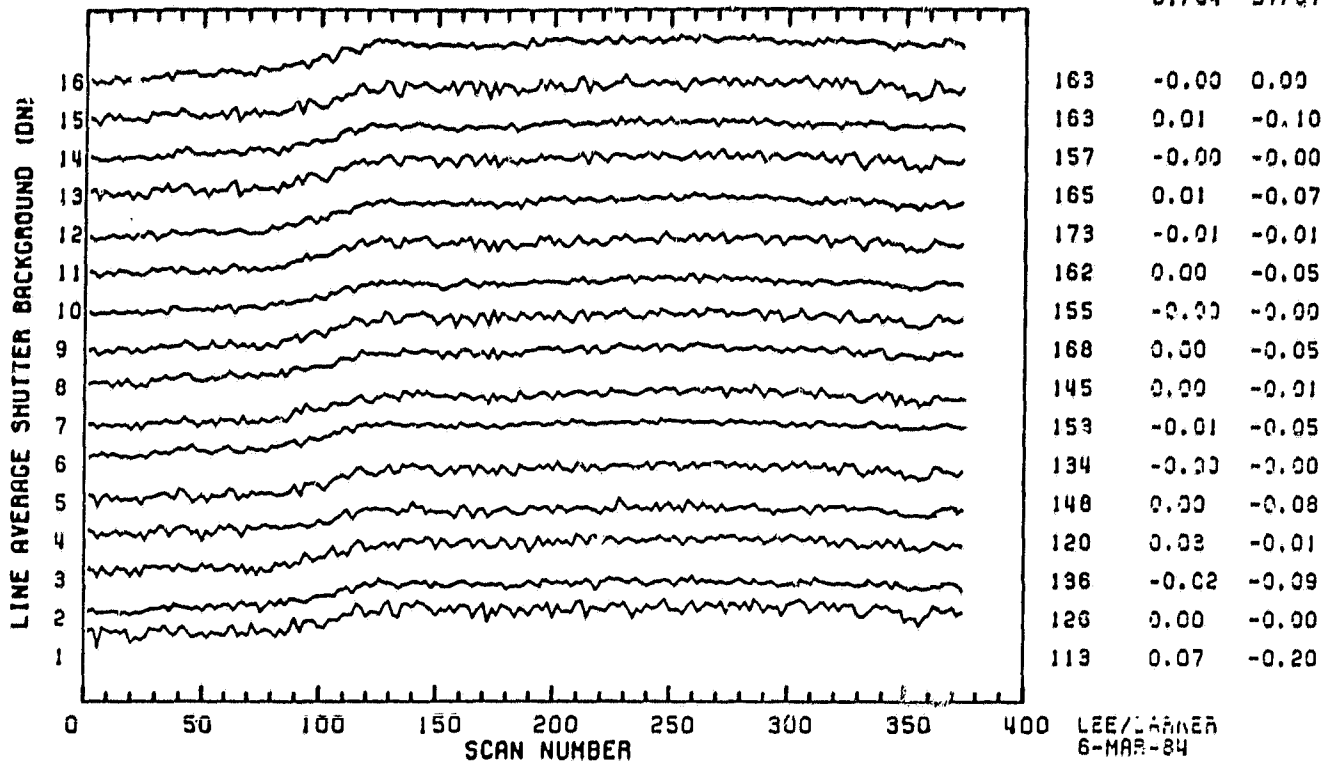


FIGURE 7.

ORIGINAL PALETTE
OF POOR QUALITY

SCENE 10-40392-18152, BAND 2 (FORWARD)
SHUTTER BACKGROUND 2 SPECTRA AFTER CORRECTION



SCENE 10-40392-18152, BAND 2 (REVERSE)
SHUTTER BACKGROUND 2 SPECTRA AFTER CORRECTION

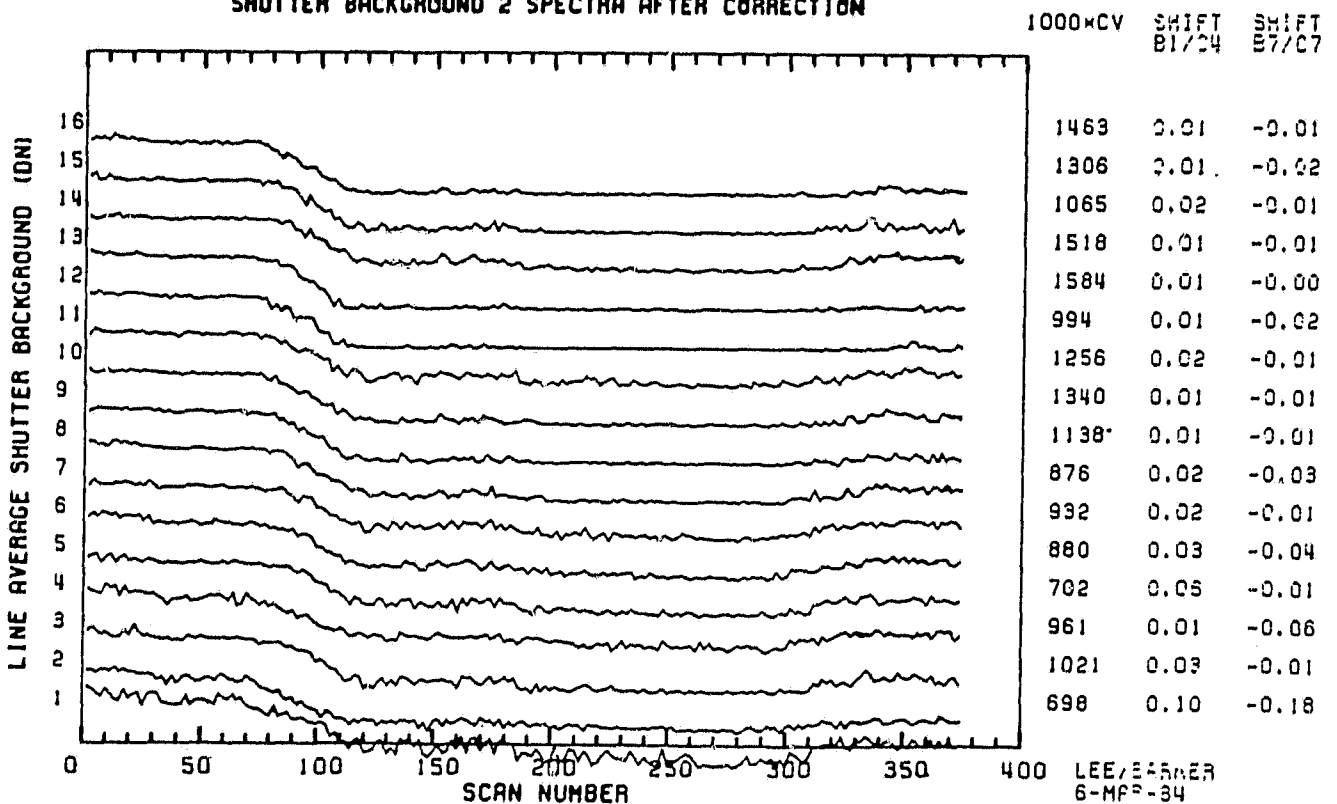


FIGURE 8.

LANDSAT-4 TM RADIOMETRY, BAND 2 CHANNEL 14

BRIGHT TARGET SATURATION OF SCENE 40392-18152

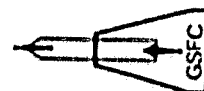
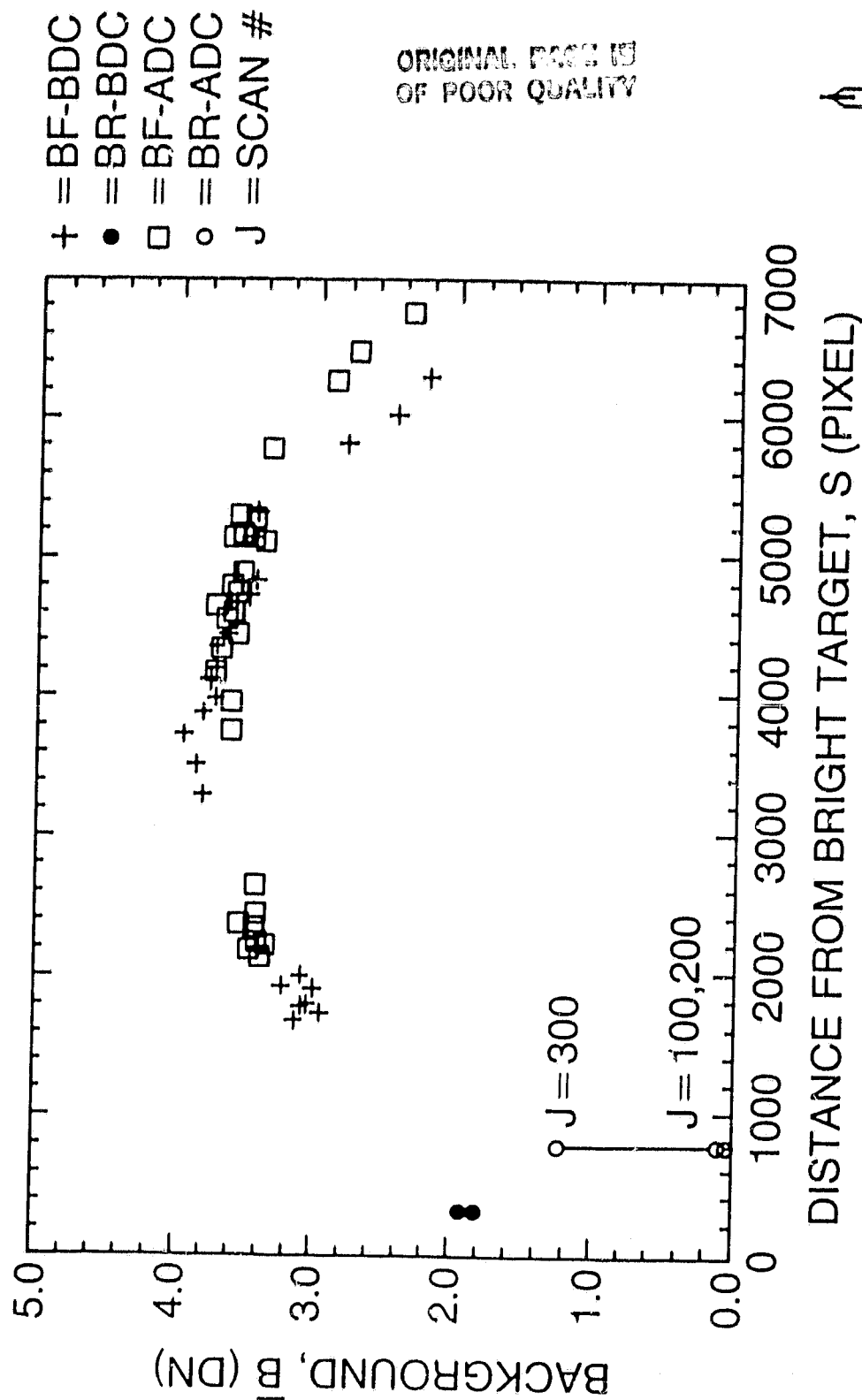


TABLE 7.

BAND 1 ON LANDSAT-4 TM/PF, WITHIN- SCENE VARIABILITY (IN DN)

TOTAL VARIABILITY				(FWD-REV) DIFFERENCE		SCAN-CORRELATED		COHERENT NOISE		
STANDARD DEVIATION OF SHUTTER IN AND AROUND DC RESTORATION				BACKGROUND ON SHUTTER IN AND AROUND DC RESTORATION		SHIFTS				
CHANNEL	PM SCENE ^a SD(B)	CLOUDY SCENE ^b		PM SCENE ^a ΔBFR	CLOUDY SCENE ^b		TYPE 4-1.4 AVERAGE ^b CS(4-1)	TYPE 4-7.7 AVG ^{a,b} CS (4-7)	32 KHz (3.2 mlf) (area ±2 mlf of peak) CC (32)	6 KHz ^c (18 mlf) CC(6)
		SD(B-BDC)	SD(B-ADC)		ΔBFR (BDC)	ΔBFR (ADC)				
16	±1.5	±1.7	±1.7	0.1	-0.6	1.2	0.1	0.0	2.6	0.2
15	±1.4	±1.5	±1.6	0.3	-0.1	2.5	0.0	0.1	1.0	0.3
14	±1.3	±1.5	±1.4	0.1	-0.6	1.6	0.2	0.0	1.7	0.2
13	±1.3	±1.4	±1.4	0.3	-0.2	2.0	0.1	0.1	0.8	0.3
12	±1.1	±1.6	±1.4	0.2	-0.4	1.3	1.7	0.0	0.9	0.4
11	±1.3	±1.4	±1.4	0.3	-0.4	2.0	0.0	-0.1	1.0	0.2
10	±1.0	±1.4	±1.4	0.1	0.6	1.8	1.0	0.0	0.6	0.3
9	±1.1	±1.2	±1.2	0.2	-0.5	1.4	0.0	0.0	0.7	0.2
8	±1.2	±1.5	±1.5	0.1	-1.1	1.3	0.8	-0.1	1.8	0.1
7	±1.3	±1.4	±1.3	0.2	-0.5	1.4	0.0	-0.1	0.6	0.4
6	±1.3	±1.6	±1.5	0.1	-1.3	1.2	0.2	0.0	1.1	0.2
5	±1.1	±1.2	±1.0	0.2	-0.4	1.0	0.0	0.1	1.1	0.3
4	±1.2	±1.8	±1.6	0.2	-0.5	1.6	2.0	0.0	0.3	0.4
3	±1.1	±1.2	±1.2	0.2	-0.6	1.4	0.0	-0.1	1.2	0.4
2	±1.3	±1.6	±1.6	0.2	-0.7	1.7	0.1	-0.1	1.6	0.1
1	±1.3	±1.4	±1.3	0.2	-0.4	1.3	0.3	-0.1	1.0	0.4

^aPM BUFFALO, NY (40037-02243), ^bSAN FRANCISCO, CA (40392-18152), ^cWHITE SANDS, NM (40171-17080)



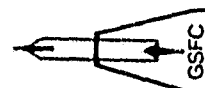
2ARKER APR 84

TABLE 8.

BAND 2 ON LANDSAT-4 TM/PF, WITHIN- SCENE VARIABILITY (IN DN)

CHANNEL	TOTAL VARIABILITY				(FWD-REV) DIFFERENCE		SCAN-CORRELATED		COHERENT NOISE		
	STANDARD DEVIATION OF SHUTTER IN AND AROUND DC RESTORATION				BACKGROUND ON SHUTTER IN AND AROUND DC RESTORATION		SHIFTS				
	CLOUDY SCENE ^b				CLOUDY SCENE ^b		TYPE 4-1.4 AVERAGE ^b CS (4-1)	TYPE 4-7.7 AVG ^{a,b} CS (4-7)	32 KHz (3.2 mf) {area ± 2 mf of peak}	6 KHz (18 mf)	CC (6)
	PM SCENE ^a SD(B)	SD(B-BDC)	SD(B-ADC)	PM SCENE ^a Δ BFR	Δ BFR (BDC)	Δ BFR (ADC)					
16	± 0.5	± 1.7	± 1.6	0.1	1.5	2.3	0.0	0.0	0.2	0.1	
15	± 0.6	± 1.5	± 1.5	0.3	1.3	2.6	0.0	0.0	0.1	0.1	
14	± 0.4	± 1.5	± 1.5	0.1	1.2	2.5	0.0	0.0	0.1	0.0	
13	± 0.6	± 1.4	± 1.6	0.3	1.5	2.8	0.0	0.0	0.1	0.1	
12	± 0.5	± 1.6	± 1.5	0.2	1.3	2.7	0.0	0.0	0.2	0.0	
11	± 0.5	± 1.4	± 1.4	0.3	1.3	2.4	0.0	0.0	0.1	0.0	
10	± 0.4	± 1.4	± 1.4	0.1	1.2	2.5	0.0	0.0	0.1	0.0	
9	± 0.5	± 1.2	± 1.5	0.2	1.3	2.6	0.0	0.0	0.0	0.0	
8	± 0.5	± 1.5	± 1.5	0.1	1.3	2.7	0.0	0.0	0.2	0.0	
7	± 0.5	± 1.4	± 1.4	0.2	1.2	2.3	0.0	0.0	0.1	0.1	
6	± 0.5	± 1.6	± 1.5	0.1	1.3	2.7	0.0	0.0	0.3	0.1	
5	± 0.5	± 1.2	± 1.4	0.2	1.3	2.4	0.0	-0.1	0.2	0.1	
4	± 0.7	± 1.8	± 1.4	0.2	1.1	2.2	0.1	0.0	0.1	0.1	
3	± 0.6	± 1.2	± 1.5	0.2	1.3	2.6	0.0	-0.1	0.2	0.1	
2	± 1.0	± 1.6	± 1.7	0.2	1.1	2.6	0.0	0.0	0.3	0.1	
1	± 0.7	± 1.4	± 1.5	0.2	1.3	2.6	0.1	-0.2	0.2	0.2	

^aPM BUFFALO, NY (40037-02243), ^bSAN FRANCISCO, CA (40392-18152), ^cWHITE SANDS, NM (40171-17080)



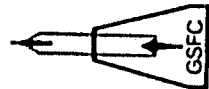
BARKER APR 84

TABLE 9.

BAND 3 ON LANDSAT-4 TM/PF, WITHIN- SCENE VARIABILITY (IN DN)

CHANNEL	TOTAL VARIABILITY				(FWD-REV) DIFFERENCE		SCAN- CORRELATED		COHERENT NOISE		
	STANDARD DEVIATION OF SHUTTER IN AND AROUND DC RESTORATION				BACKGROUND ON SHUTTER IN AND AROUND DC RESTORATION		SHIFTS				
	PM SCENE ^a SD(B)	CLOUDY SCENE ^b			PM SCENE ^a Δ BFR	CLOUDY SCENE ^b		TYPE 4-1.4 AVERAGE ^b CS(4-1)	TYPE 4-7.7 AVG ^{a,b} CS (4-7)	32 KHz (3.2 mf) (area ± 2 mf of peak) CC (32)	6 KHz (18 mf) CC(6)
16	± 1.0	± 1.5	± 1.6		0.1	Δ BFR (BDC)	Δ BFR (ADC)	0.1	0.6	0.9	0.3
15	± 0.9	± 1.4	± 1.4		0.2	1.3	2.7	0.2	0.3	0.2	0.3
14	± 0.5	± 1.2	± 1.6		0.0	1.4	2.3	0.0	0.0	0.4	0.1
13	± 0.8	± 1.3	± 1.4		0.2	1.6	2.7	0.1	-0.1	0.2	0.1
12	± 0.4	± 1.1	± 1.6		0.1	1.4	2.3	0.0	0.0	0.1	0.1
11	± 0.7	± 1.2	± 1.4		0.1	1.4	2.8	0.0	-0.1	0.1	0.1
10	± 0.5	± 1.1	± 1.7		0.1	1.3	2.3	0.0	0.0	0.0	0.2
9	± 0.8	± 1.3	± 1.6		0.2	1.4	3.0	0.0	0.0	0.3	0.1
8	± 0.9	± 1.2	± 1.6		0.1	1.5	2.8	0.0	0.0	0.1	0.2
7	± 0.7	± 1.2	± 1.4		0.1	1.2	2.6	0.0	0.0	1.6	0.1
6	± 0.5	± 1.0	± 1.5		0.1	1.2	2.3	0.0	-0.1	0.1	0.2
5	± 0.8	± 1.2	± 1.4		0.2	1.4	2.6	0.0	0.0	0.3	0.2
4	± 0.7	± 1.1	± 1.4		0.1	1.2	2.4	0.1	-0.2	0.1	0.1
3	± 0.8	± 1.2	± 1.2		0.2	1.0	2.2	0.0	0.0	1.2	0.2
2	± 0.6	± 1.0	± 1.3		0.1	1.1	2.0	0.1	-0.2	0.1	0.2
1	± 1.3	± 1.7	± 1.3		0.3	0.9	2.1	0.0	0.1	0.2	0.3
						1.4	2.0	0.3	0.5	0.3	0.5

^aPM BUFFALO, NY (40337-02243), ^bSAN FRANCISCO, CA (40392-18152), ^cWHITE SANDS, NM (40171-17080)



BARKER APR 84

TABLE 10.

BAND 4 ON LANDSAT-4 TM/PF, WITHIN- SCENE VARIABILITY (IN DN)

CHANNEL	TOTAL VARIABILITY				(FWD-REV) DIFFERENCE				SCAN- CORRELATED SHIFTS		COHERENT NOISE	
	STANDARD DEVIATION OF SHUTTER IN AND AROUND DC RESTORATION				BACKGROUND ON SHUTTER IN AND AROUND DC RESTORATION				TYPE 4-1.4 AVERAGE ^b CS(4-1)		TYPE 4-7.7 AVG ^{a,b} CS (4-7)	
	PM SCENE ^a SD(B)		CLOUDY SCENE ^b SD(B-BDC) SD(B-ADC)		PM SCENE ^a ΔBFR		CLOUDY SCENE ^b ΔBFR (E _{DC}) ΔBFR (ADC)		TYPE 4-1.4 AVERAGE ^b CS(4-1)		TYPE 4-7.7 AVG ^{a,b} CS (4-7)	
16	±0.3	±0.7	±0.9	±0.9	0.0	0.5	1.4	0.2	0.0	0.2	0.3	0.3
15	±0.4	±0.6	±1.1	±1.1	0.1	0.4	1.7	0.1	0.0	0.2	0.1	0.1
14	±0.3	±0.8	±1.2	±1.2	0.1	0.6	1.9	0.0	0.0	0.2	0.0	0.0
13	±0.4	±0.6	±0.8	±0.8	0.1	0.4	1.3	0.0	0.0	0.2	0.1	0.1
12	±0.3	±0.7	±1.1	±1.1	0.1	0.4	1.8	0.1	0.0	0.1	0.1	0.1
11	±0.3	±0.6	±0.9	±0.9	0.1	0.3	1.4	0.1	0.0	0.3	0.1	0.1
10	±0.3	±0.7	±1.0	±1.0	0.1	0.4	1.6	0.0	0.0	0.3	0.0	0.0
9	±0.3	±0.6	±1.1	±1.1	0.1	0.3	1.8	0.0	0.0	0.2	0.1	0.1
8	±0.6	±0.9	±1.1	±1.1	0.1	0.3	1.6	0.0	-0.1	0.8	0.1	0.1
7	±0.3	±0.6	±0.9	±0.9	0.1	0.4	1.5	0.0	0.0	0.2	0.1	0.1
6	±0.5	±0.7	±1.1	±1.1	0.1	0.4	1.8	0.0	0.0	0.3	0.1	0.1
5	±0.4	±0.7	±1.0	±1.0	0.1	0.5	1.7	0.0	0.0	0.3	0.1	0.1
4	±0.5	±0.8	±1.0	±1.0	0.1	0.2	1.6	0.0	-0.1	0.5	0.0	0.0
3	±0.6	±0.7	±1.1	±1.1	0.2	0.4	1.9	0.0	0.0	0.4	0.2	0.2
2	±0.4	±0.8	±1.1	±1.1	0.1	0.3	1.7	0.0	-0.1	0.3	0.1	0.1
1	±0.6	±0.7	±0.8	±0.8	0.1	0.5	1.3	0.2	-0.1	0.6	0.2	0.2

^aPM BUFFALO, NY (40037-02243), ^bSAN FRANCISCO, CA (40392-18152), ^cWHITE SANDS, NM (43171-17080)



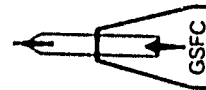
BARKER APR 84

TABLE 11.

BAND 5 ON LANDSAT-4 TM/PF, WITHIN- SCENE VARIABILITY (IN DN)

TOTAL VARIABILITY STANDARD DEVIATION OF SHUTTER IN AND AROUND DC RESTORATION				(FWD-REV) DIFFERENCE BACKGROUND ON SHUTTER IN AND AROUND DC RESTORATION			SCAN- CORRELATED SHIFTS		COHERENT NOISE	
CHANNEL	PM SCENE ^a SD(B)	CLOUDY SCENE ^b		PM SCENE ^a Δ BFR	CLOUDY SCENE ^b		TYPE 4-1.4 AVERAGE ^b CS(4-1)	TYPE 4-7.7 AVG ^{a,b} CS (4-7)	32 KHz (3.2 mf) (area ± 2 mf of peak) CC (32)	6 KHz (18 mf) CC(6)
		SD(B-BDC)	SD(B-ADC)		Δ BFR (BDC)	Δ BFR (ADC)				
16	± 0.8	± 0.9	± 0.8	0.1	0.3	0.2	0.0	0.1	[0.2]	[0.1]
15	± 0.9	± 0.9	± 0.9	0.1	-0.3	0.1	-0.1	0.1	[0.3]	[0.1]
14	± 0.9	± 0.9	± 0.9	0.0	-0.1	0.0	0.0	-0.1	[0.1]	[0.1]
13	± 0.9	± 0.9	± 0.9	0.0	-0.1	0.0	0.0	0.0	[0.1]	[0.1]
12	± 0.9	± 0.9	± 0.9	0.0	-0.1	0.0	0.0	0.0	[0.0]	[0.1]
11	± 0.9	± 1.0	± 0.9	0.0	-0.1	0.0	0.0	0.0	[0.0]	[0.1]
10	± 0.9	± 1.0	± 0.9	0.0	-0.1	0.0	0.0	0.0	[0.1]	[0.1]
9	± 0.9	± 0.9	± 0.9	0.0	-0.1	-0.1	0.0	0.6	[0.1]	[0.0]
8	± 0.9	± 0.9	± 0.8	0.0	-0.1	0.0	0.0	0.0	[0.0]	[0.0]
7	± 1.1	± 1.1	± 1.1	0.0	-0.1	0.0	0.0	-0.2	[0.2]	[0.0]
6	± 0.9	± 0.9	± 0.9	0.0	-0.1	0.0	0.0	0.1	[0.2]	[0.2]
5	± 0.9	± 0.9	± 0.9	0.0	-0.1	-0.1	-0.1	-0.1	[0.2]	[0.0]
4	± 0.8	± 0.9	± 0.9	0.0	-0.1	0.0	0.1	0.0	[0.1]	[0.0]
3	—	—	—	—	—	—	0.0	0.0	—	—
2	± 0.8	± 0.9	± 0.8	0.1	-0.7	-0.1	0.1	-0.1	[0.1]	[0.1]
1	± 0.8	± 0.9	± 0.9	0.0	-0.7	-0.1	0.0	0.1	[0.2]	[0.0]

^aPM BUFFALO, NY (40037-02243), ^bSAN FRANCISCO, CA (40392-18152), ^cWHITE SANDS, NM (40171-17080)



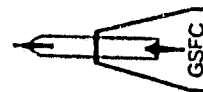
BARKER APR 84 GSFC

TABLE 12.

BAND 7 ON LANDSAT-4 TM/PF, WITHIN- SCENE VARIABILITY (IN DN)

TOTAL VARIABILITY				(FWD-REV) DIFFERENCE			SCAN- CORRELATED SHIFTS		COHERENT NOISE	
STANDARD DEVIATION OF SHUTTER IN AND AROUND DC RESTORATION				BACKGROUND ON SHUTTER IN AND AROUND DC RESTORATION						
CHANNEL	PM SCENE ^a SD(B)	CLOUDY SCENE ^b		PM SCENE ^a ΔBFR	CLOUDY SCENE ^b		TYPE 4-1.4 AVERAGE ^b CS(4-1)	TYPE 4-7.7 AVG ^{a,b} CS (4-7)	32 KHz (3.2 mf) (area = 2 mf of peak) CC (32)	6 KHz (18 mf) CC(6)
		SD(B-BDC)	SC(B-ADC)		ΔBFR (BDC)	ΔBFR (ADC)				
16	±1.0	±1.0	±1.0	0.1	-0.2	0.2	0.1	0.2	[0.2]	[0.1]
15	±0.8	±0.8	±0.8	0.1	0.2	0.1	0.0	0.2	[0.1]	[0.2]
14	±1.1	±1.1	±1.1	0.0	0.1	0.0	0.1	0.1	[0.0]	[0.1]
13	±0.8	±0.9	±0.8	0.0	0.1	0.0	0.0	0.2	[0.1]	[0.1]
12	±1.0	±1.0	±1.0	0.0	0.0	0.0	0.1	0.2	[0.2]	[0.1]
11	±1.0	±1.0	±0.9	0.0	0.0	0.0	0.0	0.2	[0.1]	[0.0]
10	±1.1	±1.1	±1.1	0.0	0.0	0.0	0.1	0.4	[0.3]	[0.0]
9	±1.0	±1.0	±1.0	0.0	-0.1	0.0	0.1	0.2	[0.1]	[0.0]
8	±1.0	±1.0	±0.9	0.0	0.1	0.0	0.0	0.3	[0.1]	[0.1]
7	±2.0	±1.8	±1.8	0.0	0.2	0.2	0.1	0.9	[0.1]	[0.2]
6	±1.0	±1.0	±1.0	0.0	0.0	0.0	0.1	0.3	[0.1]	[0.1]
5	±0.9	±1.0	±0.9	0.0	0.0	0.0	0.0	0.2	[0.0]	[0.1]
4	±1.0	±1.0	±1.0	0.0	-0.1	0.0	0.1	-0.2	[0.2]	[0.1]
3	±0.9	±0.9	±0.9	0.0	0.1	0.0	0.1	0.3	[0.1]	[0.0]
2	±1.0	±1.0	±1.0	0.1	-0.6	0.1	0.0	0.3	[0.2]	[0.1]
1	±1.0	±1.0	±1.0	0.0	-0.6	0.1	0.0	0.3	[0.1]	[0.1]

^aPM BUFFALO, NY (40037-02243), ^bSAN FRANCISCO, CA (40392-18152), ^cWHITE SANDS, NM (40171-17080)



BARKER APR 84

TABLE 13.

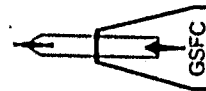
LANDSAT-5 TM/F WITHIN-SCENE VARIABILITY (IN DN)

CHANNEL	BAND 1			BAND 2			BAND 3			BAND 4			BAND 5			BAND 7		
	TOTAL SHUTTER NOISE ^a SD(B)	SHIFT TYPE 5-3.1 AVERAGE ^b CS (5-3)	TOTAL SHUTTER NOISE ^a SD(B)	SHIFT TYPE 5-3.1 AVERAGE ^b CS (5-3)	TOTAL SHUTTER NOISE ^a SD(B)	SHIFT TYPE 5-3.1 AVERAGE ^b CS (5-3)	TOTAL SHUTTER NOISE ^a SD(B)	SHIFT TYPE 5-3.1 AVERAGE ^b CS (5-3)	TOTAL SHUTTER NOISE ^a SD(B)	SHIFT TYPE 5-3.1 AVERAGE ^b CS (5-3)	TOTAL SHUTTER NOISE ^a SD(B)	SHIFT TYPE 5-3.1 AVERAGE ^b CS (5-3)	TOTAL SHUTTER NOISE ^a SD(B)	SHIFT TYPE 5-3.1 AVERAGE ^b CS (5-3)	TOTAL SHUTTER NOISE ^a SD(B)	SHIFT TYPE 5-3.1 AVERAGE ^b CS (5-3)	TOTAL SHUTTER NOISE ^a SD(B)	SHIFT TYPE 5-3.1 AVERAGE ^b CS (5-3)
16	± 0.9	0.2	± 0.3	0.7	± 0.5	0.3	± 0.5	0.3	± 0.5	0.3	± 0.8	0.0	± 0.9	0.0	± 0.9	± 0.9	± 0.9	± 0.9
15	± 0.8	0.0	± 0.3	0.3	± 0.4	0.3	± 0.4	0.3	± 0.3	0.1	± 0.8	0.1	± 0.8	0.1	± 0.8	± 0.8	± 0.8	± 0.8
14	± 1.0	0.3	± 0.2	0.2	± 0.4	0.3	± 0.4	0.3	± 0.4	0.0	± 0.8	0.0	± 0.8	0.0	± 0.8	± 0.9	± 0.9	± 0.9
13	± 0.8	0.0	± 0.3	0.4	± 0.5	0.3	± 0.5	0.3	± 0.3	0.2	± 0.9	0.2	± 0.9	0.2	± 0.8	± 0.8	± 0.8	± 0.8
12	± 0.9	0.2	± 0.2	0.1	± 0.7	0.3	± 0.7	0.3	± 0.3	0.0	± 1.0	0.0	± 1.0	0.0	± 1.0	± 1.0	± 1.0	± 1.0
11	± 0.9	0.0	± 0.3	0.3	± 0.5	0.5	± 0.5	0.5	± 0.4	0.1	± 0.8	0.1	± 0.8	0.1	± 0.8	± 0.9	± 0.9	± 0.9
10	± 0.9	-0.3	± 0.2	0.0	± 0.4	0.4	± 0.4	0.4	± 0.3	0.0	± 1.3	0.0	± 1.3	0.0	± 1.3	± 1.0	± 1.0	± 1.0
9	± 0.8	0.0	± 0.3	0.2	± 0.6	0.4	± 0.6	0.4	± 0.4	0.1	± 1.0	0.1	± 1.0	0.1	± 1.3	± 1.3	± 1.3	± 1.3
8	± 1.0	-0.1	± 0.2	0.1	± 0.5	0.2	± 0.5	0.2	± 0.4	0.0	± 0.9	0.0	± 0.9	0.0	± 1.0	± 1.0	± 1.0	± 1.0
7	± 0.8	0.0	± 0.3	0.3	± 0.5	0.3	± 0.5	0.3	± 0.3	0.1	± 0.9	0.1	± 0.9	0.1	± 0.9	± 0.9	± 0.9	± 0.9
6	± 0.9	-0.1	± 0.2	0.1	± 0.4	0.6	± 0.4	0.6	± 0.4	0.0	± 0.8	0.0	± 0.8	0.0	± 0.8	± 0.9	± 0.9	± 0.9
5	± 0.8	0.0	± 0.3	0.3	± 0.6	0.4	± 0.6	0.4	± 0.3	0.1	± 0.9	0.1	± 0.9	0.1	± 0.8	± 0.8	± 0.8	± 0.8
4	± 1.0	-0.1	± 0.3	0.0	± 0.5	0.5	± 0.5	0.5	± 0.4	0.3	± 0.9	0.3	± 0.9	0.3	± 0.9	± 0.9	± 0.9	± 0.9
3	± 0.9	0.0	± 0.4	0.4	± 0.6	0.5	± 0.6	0.5	± 0.5	0.1	± 0.9	0.1	± 0.9	0.1	± 0.9	± 0.9	± 0.9	± 0.9
2	± 1.0	-0.1	± 0.4	0.0	± 0.5	0.2	± 0.5	0.2	± 0.4	0.1	± 0.8	0.1	± 0.8	0.1	± 0.8	± 1.0	± 1.0	± 1.0
1	± 1.0	0.0	± 0.5	0.7	± 0.6	0.5	± 0.6	0.5	± 0.2	0.4	± 0.8	0.4	± 0.8	0.4	± 0.8	± 0.9	± 0.9	± 0.9

^aPRE-LAUNCH "IS GOLDEN TAPE" (5-198-10563, 16:14 30 AUG 83)

^bAVERAGED (5-596-13285), (5-198-10563) AND (50005-16221)

ORIGINAL PAGE IS
OF POOR QUALITY



BARKER APR 84

the Landsat Project. Evaluation, and possible implementation, of the recommendations will pose significant difficulties both during the research period before the transition of the TIPS from NASA to NOAA near the end of 1984, and afterwards, during the operational period.

TABLE 14
RECOMMENDATIONS
TM RADIOMETRIC CHARACTERIZATION

6.1 ENGINEERING CHARACTERIZATION

6.1.1 RECALIBRATE INTEGRATING SPHERE USED IN PRE-LAUNCH
CALIBRATION

- 48" TM Integrating Sphere
 - SBRC
 - GSFC
 - NBS
- Two 30" MSS Spheres
- MMR 8-Band Field Radiometer

6.1.2 ANALYZE RELATIVE RADIOMETRY OF PRE-LAUNCH DATA ON 42 TRACK
TAPES

6.1.3 EMPLOY ENGINEERING MODEL TM TESTS TO INVESTIGATE SOURCE OF

- Bin-Radiance Dependence (Unequal Bins)
- Coherent Noise (Stationary and Time-Dependent)
- Within-Line Droop
- Bright Target Saturation (Recovery)
- Scan-Related Shifts
- IC Pulse Temperature-Dependence
- "Secondary" Light Pulse in Calibration Region
- Apparent Gain Changes with Time

6.1.4 PRODUCE FINAL REPORT DESCRIBING TM PERFORMANCE
CHARACTERISTICS

6.2 FLIGHT SEGMENT OPERATIONS

6.2.1 INSTITUTE CHANGES IN OPERATIONAL PROCEDURES

- Stop Routine Operation of IC Automatic Sequencer
- Alternate Black Body Temperatures "T2" and "T3"
- Set Outgassing Strategy at 20% Band 6 Gain Loss

6.2.2 PERFORM IN-ORBIT CALIBRATION TESTS

- Calibrate Temperature-Dependence of IC Pulses

6.2.3 PERFORM IN-ORBIT CHARACTERIZATION TESTS

- Redundant Power Supply Noise
- Manual IC Operation with Automatic Sequencer Off
- "Override" Back-up IC Operation
- Coherent Noise Phasing Relative to Midscan Pulse
- Noise with DC Restoration Off

6.2.4 PERFORM IN-ORBIT SCIENTIFIC MISSION TESTS

- Subsampled Extension of Swath Width, No Shutter
- Bidirectional Reflectance by Off-Nadir Pointing
- Intensive Single Site Acquisition by Pointing
- TM/F and TM/PF Stereo by Pointing
- TM/F and MSS/F (High Gain) Bathymetry
- TM Single S/C Stereo
 - Fore/Aft
 - Side-to-Side

6.3 TIPS GROUND PROCESSING

6.3.1 PROVIDE FOR FUTURE CHANGE IN RADIOMETRIC CALIBRATION PARAMETERS

- Post-Calibration Dynamic Range (RMIN, RMAX)
- Spectral Radiance for each IC Lamp Level
- Averaged Pulse for each IC Lamp Level
- Pre-Launch Gains and Offsets
- Calculated Pre-Launch Nominal IC Pulses

6.3.2 PROVIDE FOR CHANGES IN IC SYSTEMATIC RADIOMETRIC CORRECTION PROCEDURES INVOLVING

- Two Background Shutter Collects (avoid DC Restore)
- Within-Scene Corrections
 - Bin-Radiance Dependence
 - Coherent Noise
 - Scan-Related Shifts
- Background Outliers (Incomplete Obscuration)
- "Secondary" Light Pulses in Calibration Region
 - Search 80 of 148 mf Collect Window
- Pulse Integration Parameters
 - Optimize Integration Width (near 39 mf)
- Pulse Averaging
 - Separate Forward and Reverse Scans
- Lamp State Options
 - Reject 111 State for any Regression
 - Omit 000 State when possible
 - Omit Shutter Background when possible
 - Permit any States and Background
- IC Pulse Temperature-Dependence
- Between-Channel Correlations
 - Between-Band Absolute Radiometry
 - Quality Assurance Redundancy Check
- Within-Pass Smoothing
- Between-Date Smoothing
- Reference Channels or Variance Weighting
- Statistical Quality Indices

6.3.3 MODIFY HISTOGRAM EQUALIZATION PROCEDURE TO PROVIDE FOR

- Optional 1st Pass HDT-RT Histogram
- Line-by-line Systematic Correction
- 2nd Pass HDT-RT 11-Bit Histogram
- HDT-AT 11-Bit Histogram and File
- Histogram Reference to "Quiet" Channel
- Histogram Monitoring of IC quality
- Weighting of IC and Histogram Constants
- HDT-PT Histogram File for each Band

- 6.3.4 MODIFY GEOMETRIC PROCESSING PROCEDURES TO PROVIDE FOR
- Single Pass Image Rectification (Geodetic) Product
 - Geocoded Map Compatibility
 - UTM Resampling as Standard
 - Single Pass Cubic Spline Resampling
 - Image Coordinate File for GCPs
 - Relative GCPs
 - Alternative Global GCP Library Build
- 6.3.5 PROVIDE THREE-SECTIONED POST-CALIBRATION DYNAMIC RANGE
- 6.3.6 MODIFY IMAGE CALIBRATION PROCEDURE TO PROVIDE FOR
- Non-Adjacent Channel Replacement Algorithm
 - Probabilistic Approach
- 6.3.7 PROVIDE THE FOLLOWING PRODUCTS
- Semi-weekly Tapes of Raw Calibration Data
 - Semi-weekly "Unity" CCT-AT
 - Special "Unity" CCT-AT of Calibration Region
 - Reprocessed "Reference" Scenes
 - History Tapes of Calibration Constants
 - Selected HDT-RT Copies
 - Extra Band(s) of Binary Data
 - Extra Band(s) of 8-Bit Data
 - Tapes at Reduced Resolution
 - Cloud-free Global TM Archive by Season
 - "Unity" HDT-AT and CCT-AT as Standard, with PDC
- 6.3.8 RESEARCH AND DEVELOP PROCEDURES FOR
- Within-Line Processing
 - Band 6 Processing
 - Ingestion of Foreign TM Tapes
 - Full Interval Radiometric Processing
 - Creation and Processing of Pre-Launch Data
 - GPC Test to Reduce Control Point Neighborhood Size

6.4

DEVELOP PROCEDURES FOR POSSIBLE CONTINGENCY EXPERIMENTS

- SCIENTIFIC EXPERIMENTS

- Lunar Radiometric Calibration
- Stereo and Bidirectional Reflectance
- Time-of-Day Orbital Changes
- Revisit Frequency Requirements
- Utility of Mixed Spatial Resolution

- ENGINEERING EXPERIMENTS

- Band 6 Sensitivity at 70K
- Focus Test on Inchworms over GCPs
- Tests of Global Position System Utility
- Tests of On-Board Computer Options
- Alternative Lamp and Power Supply Tests
- Recalibration Before and After In-Orbit Repair